J Exp Biol Advance Online Articles. First posted online on 23 December 2016 as doi:10.1242/jeb.146076
Access the most recent version at http://jeb.biologists.org/lookup/doi/10.1242/jeb.146076

The energetic cost of filtration by demosponges and their behavioural response to ambient currents

Ludeman, Danielle A[1]
Reidenbach, Matthew A[2]
Leys, Sally P[1*]

*correspondence: sleys@ualberta.ca

[1]Department of Biological Sciences, University of Alberta, CW 405 Biological Sciences Building, Edmonton, Alberta T6G 2E9, Canada.

[2]Department of Environmental Sciences, University of Virginia, 291 McCormick Rd, Clark Hall, Charlottesville, Virginia, 22904, USA.

Keywords

Porifera; filter feeding; passive flow; current-induced flow; oxygen; energetic cost

Summary Statement

Filter feeding in demosponges is energetically costly, with some species showing active behavioural control over the amount of water they filter under different ambient current speeds.

Abstract

Sponges (Porifera) are abundant in most marine and freshwater ecosystems and as suspension feeders they play a crucial role in filtering the water column. Their active pumping enables them to filter up to 900 times their body volume of water per hour, recycling nutrients and coupling a pelagic food supply with benthic communities. Despite the ecological importance of sponge filter feeding, little is known about how sponges control the water flow through their canal system or how much energy it costs to filter the water. Sponges have long been considered textbook examples of animals that use current-induced flow. We provide evidence which suggests that some species of demosponge do not use current-induced flow, rather they respond behaviourally to increased ambient currents by reducing the volume of water filtered. Using a morphometric model of the canal system, we also show that filter feeding may be more energetically costly than previously thought.

Journal of Experimental Biology • Advance article

Measurements of volumetric flow rates and oxygen removal in five species of demosponge show that pumping rates are variable within and between species, with more oxygen consumed the greater the volume filtered. Together these data suggest that sponges have active control over the volume of water they process, which may be an adaptation to reduce the energetic cost of filtration in times of high stress.

Introduction

Benthic suspension feeders affect marine and freshwater ecosystems by ingesting suspended particulates and dissolved nutrients from the overlying water column and releasing by-products for use by other organisms (Gili and Coma, 1998). Recycling of nutrients in this way provides an important link between the benthic and pelagic communities, known as benthic-pelagic coupling, yet the energetic cost of this type of feeding in invertebrates is still debated. Some work suggests the cost of pumping for filtration is minimal (Riisgård and Larsen, 1995; Riisgård and Larsen, 2001), while other studies estimate that filtration can make up a quarter of the costs of metabolism (Hadas et al., 2008).

Many suspension feeders use ciliary or muscular pumps to induce water currents that draw water with food towards themselves. Bivalves, ascidians, polychaetes and sponges use filters to strain out particles from the water that are too small to be captured individually (Jørgensen, 1966). Where suspended particulates are low in concentration, this approach can be highly efficient to process large volumes of water (Jørgensen, 1966), and so it has been suggested that filter feeders evolved a low energetic cost of filtration to allow continuous feeding (Jørgensen, 1975). Yet, food availability varies widely on a temporal basis, with fluctuations occurring seasonally, daily, and with the ebb and flood of the tide. It would therefore be advantageous for filter feeders to sense the variations in food availability and feed when concentrations are high. Two examples suggest this behaviour does occur. Bivalves respond to food availability by reducing filtration and respiration rates when food is scarce (Griffiths and King, 1979; Thompson and Bayne, 1972), and the demosponge *Tethya crypta* reduces pumping activity at night when ambient currents are lower (Reiswig, 1971); lower ambient currents often correspond with reduced food availability (Newell and Branch, 1980). As all filter feeders demonstrate some fluctuations in pumping rates in response to variations in environmental cues, filtration may be more costly than previously thought and the animals may be finely adapted to habitats that support the energetic cost to obtain food.

Models of the filter and pump system for a number of invertebrates have suggested that filter feeding is inexpensive, at less than 4% of total metabolism (Riisgård and Larsen,

Journal of Experimental Biology • Advance article

1995). In contrast, direct measurements of the uptake of oxygen going from non-feeding to feeding has shown that in bivalves filtration accounts for up to 50% of total metabolism (Newell and Branch, 1980; Thompson and Bayne, 1972) and in sponges 25% of total respiration (Hadas et al., 2008). In addition, the resistance through the filter of sponges may be much higher than previously thought due to the narrow dimensions of a difficult to preserve fine mucus mesh on the collar filter (Leys et al., 2011).

In support of the theory that the cost of filtration may be high, some animals have been found to reduce the energy expended by using ambient currents to draw water through the filter, for example by dynamic pressure, the Bernoulli Effect or viscous entrainment. In high current environments barnacles switch from active to passive feeding and orient their bodies toward the current (Trager et al., 1990). Cnidarians (Best, 1988), ascidians (Knott et al., 2004; Young and Braithwaite, 1980), and brachiopods (LaBarbera, 1977) also orient their bodies to the current, while other invertebrates may take advantage of current-induced flow through tubes (Murdock and Vogel, 1978; Shiino, 2010; Vogel, 1977; von Dassow, 2005). Sponges are often considered textbook examples of the use of current-induced flow in nature (Bidder, 1923; Vogel, 1974; Vogel, 1977) but experiments to confirm this have been equivocal (Leys et al., 2011).

Even if models are correct and cost of filtration is not great, a universal cost for all sponges is unlikely since structural differences in the sponge canal system due to body form (Reiswig, 1975a), microbial content (Weisz et al., 2008), and tissue density (Turon et al., 1997) can cause wide differences in filtration rates between species. Temperature and food availability vary across habitats causing differences in seawater viscosity and enzyme function that potentially leads to differences in the metabolic cost of filtering in different habitats. Estimates of the cost of pumping for a range of sponge species and habitats are therefore required to better understand sponge energy budgets.

Models can be informative about which structures contribute most to energetic costs, however, their accuracy depends on having correct dimensions for each region of the filter and canal system as well as volumetric flow rates. This approach used by Riisgård et al. (1993) was recently used for the filtration system of the glass sponge *Aphrocallistes vastus* (Leys et al., 2011) where the cost of pumping was found to be 28% of the total metabolism. Here, the resistance through the filter was found to be much higher than previous estimates for demosponges due to the small spaces of the glycocalyx mesh (Leys et al., 2011), a structure that is often not preserved with common fixation techniques and was not included in the model used by Riisgård et al (1993). In addition, the volumetric flow rate in *A. vastus* was

quite high compared to the 'standard sponge' studied by Riisgård et al. (1993) where volumetric flow rate was obtained indirectly using clearance rates of particles (flagellate cells) during incubation in a closed vessel. Closed vessels have been shown to cause reduced pumping behaviour of sponges (Hadas et al., 2008; Yahel et al., 2005), and the sponge may re-filter the water if sampling times are not well adjusted to pumping rates (Yahel et al., 2005). In contrast, Leys et al. (2011) used direct sampling of incurrent and excurrent water to determine filtration and pumping rates *in situ*.

To evaluate the importance of accurate measures of filter dimensions and volume of water processed when estimating the cost of filtration, we first examined the effect of changes in these values calculated in previous work. We then studied energetics of filtration in five species of demosponge from tropical and temperate habitats using *in situ* measurements of oxygen consumption and pumping rate, experimental tests of pumping at different ambient flow rates, and by morphometric analysis of the canal and filter structures.

Methods

Meta-Analysis

We first carried out a meta-analysis using data from the literature to determine the cost of pumping in four filter feeding invertebrate groups used by Riisgård and colleagues (Riisgård and Larsen, 1995). Dimensions were calculated from electron micrographs of mucus filters (Supplementary Information Figure S1), where available, and volume flow rates that were obtained using 'direct' methods were used.

Field and lab studies

Field work was carried out at the Bamfield Marine Sciences Centre (BMSC) in Bamfield, British Columbia, Canada, and the Smithsonian Tropical Research Institute (STRI) on Isla Colon in Bocas del Toro, Panama. At BMSC three species of demosponge, *Neopetrosia problematica* (N=7), *Haliclona mollis* (N=10), and *Tethya californiana* (N=8), were collected by SCUBA from Barkley Sound and kept in seawater tables at 8-9°C with unfiltered water from 30 m depth at flow rates of 3000 L min^{-1}.

Measurements on *Cliona delitrix* (N=8) and *Callyspongia vaginalis* (N=11) were conducted *in situ* by snorkeling at STRI point, GPS coordinates 9°21.169'N 82°15.528'W (Diaz, 2005) at approximately 2 m depth where seawater was 28-29°C. An aluminum frame ('80/20' Inc., Columbia City, IN) was placed over the sponge and instruments were attached

using loc-line (Lockwood Products, OR) and clamps (Figure 1). The instruments were tethered via cables to a laptop computer on a boat anchored near the study site to monitor the data collection in real time.

Measurements of excurrent velocity

Excurrent velocity was measured using a Vectrino II profiling acoustic Doppler velocimeter (ADV, Nortek), which provided 30 velocity estimates in 1 mm vertical bins, within a sampling diameter of approximately 6 mm. Because the sampling volume is some distance from the probe head, and because the excurrent 'jet' from a sponge osculum may be small, and may not travel very far from the osculum lip, positioning it over the sponge osculum is challenging. Fluorescein dye diluted in 0.2µm filtered seawater was used to visualize the excurrent flow (Supplementary Information Figure S2), and a plastic cable tie was used to indicate the specific position of the sampling volume by blocking the signal. However, the profiling capabilities of the Vectrino II also helps because it takes measurements over the full 30 mm vertical profile, and as a result the lip of the sponge osculum itself disrupts the profile, showing exactly where above the sponge the sampling volume is (Supplementary Information Figure S2). Using this method it is possible to be sure that the velocity being recorded is just inside the sponge osculum, and this becomes important in preventing interference with ambient water velocities. For the three temperate sponge species the sample volume diameter (6 mm) was greater than the diameter of the oscula and therefore the profiler captured the average velocity across the full osculum. For the two warm water sponges however, the sampling volume was smaller than the osculum diameter. However because we sampled just inside the osculum, and because ambient flow could be seen to affect scalar (x,y,z) velocity (Denny, 1993) (Supplementary Information Table S1), we therefore only used the Z velocity vector as a conservative measure of the average excurrent velocity of each osculum.

The ADV sensor was attached to loc-line for fine positioning above the sponge osculum to obtain the position of maximum excurrent velocity. Once the sensor was oriented correctly, excurrent velocity was recorded for 5 minutes at 25 Hz on low power (high power was strong enough to push the excurrent flow down, a process termed streaming). Data were binned using a 5 second median filter in MATLAB (vR2013b). Images of each sponge osculum were taken using a GoPro Hero2 for the duration of the recording and their diameters measured in ImageJ (v. 1.43r; NIH) to calculate volumetric flow.

Sponge volumes and surface area for each of the species were calculated by measuring the dimensions of the sponge from images taken of whole animals *in situ*, and using ImageJ (v. 1.43r; NIH). Volumes and surface areas were estimated as a cylinder (*C. vaginalis*), ellipsoid (*C. delitrix* and *H. mollis*), and sphere (*T. californiana*). When there was more than one osculum per sponge, sponge volume was calculated and divided by the number of oscula to get sponge volume/osculum. Because *C. delitrix* bores into coral, the ratio of sponge to coral skeleton in *C. delitrix* was estimated by dissolving the coral skeleton using 5% EDTA for a piece approximately 2 cm^3, or 4.5 g, and scaling up to the whole specimen using the relative immersed volumes. *N. problematica* is highly irregular in shape; therefore a combination of triangles was used to estimate volume and surface area. The ratio of sponge volume to dry weight was calculated by drying three pieces of each species at 100°C to constant weight. This ratio was then used to standardize volume flow rate to dry weight.

Measurements of oxygen consumption

Ambient and excurrent oxygen were measured using a two channel FireStingO_2 optical oxygen meter (Pyro Science, Germany) with 250 μm diameter bare fiber minisensor probes. Before positioning the excurrent sensor in the sponge osculum both probes were left in ambient water for at least 5 minutes to determine the difference in readings between the two sensors (here termed the offset value); this difference was subtracted from the difference between ambient and excurrent oxygen for all analyses. Oxygen sensors were calibrated to 100% and zero oxygen prior to experiments using air bubbled water and a solution of sodium hydrosulfite. Oxygen readings were corrected using both internal and external temperature probes directly by instrument and recorded in mg L^{-1}. In addition, the ambient and excurrent sensors were positioned at the same height in the water column, such that any temperature fluctuations were accounted for between probes. Data were collected every 1 s and binned using a 5 s median filter using MATLAB (vR2013b). Oxygen removal per hour was calculated using the volume of water filtered per hour, and standardized to per gram dry weight.

Effects of ambient current

To assess the effect of ambient current velocities on sponge excurrent flow, experiments were conducted on *C. delitrix* and *C. vaginalis* at STRI by manipulating ambient flow with an underwater aquarium pump (Eheim compact + 3000). The pump was anchored

near the sponges with a weight and the outflow directed through a 50 cm long, 10 cm diameter PVC pipe at and over the sponges following the method of Genin et al. (1994). The aquarium pump had variable speeds that could generate flow at 5 to 40 cm s^{-1} through the PVC pipe when positioned 30 cm from the sponge, as measured in a flow flume. Three flow speeds were used in experiments by setting the pump to low, medium, and high speeds. Ambient current velocity was recorded using a Vectrino I point ADV (Nortek) with a sampling volume of 6 mm by 7 mm, positioned approximately 10 cm from the sponge and perpendicular to the pump outflow (Figure 1F). The ADV could not be positioned right next to the sponge due to interference between the ADVs. Data were measured with a transmit length of 1.8 mm at 25 Hz on high power and binned using a 5 s median filter using MATLAB (vR2013b).

Paired excurrent velocities and oxygen removal were measured during experiments as described above. The profiling ADV (Nortek) was first positioned to ensure maximum excurrent velocity recordings from the osculum. Then the oxygen sensor was positioned inside the osculum, ensuring that it did not interfere with the ADV sampling volume as determined by a probe check analysis. Paired recordings were measured for 5 minutes at each flow rate (no additional flow, low, medium, and high pump setting), and this experiment was repeated three times.

A GoPro Hero2 camera with underwater dive housing was positioned on the frame above both sponges to record osculum size during the experiment; images were captured every 30 s and a ruler was positioned in one of the images for calibration. Changes in osculum area were measured using a script developed for MATLAB (vR2013b). Volume filtered was calculated using excurrent velocity and area of the osculum. The ratio of sponge volume to dry weight was used to standardize volume flow rate and oxygen removal to per gram dry weight.

Statistical analyses

All statistical analyses were completed using SigmaStat in SigmaPlot v12.5. Data were tested for normality and linearity and subsequently variables were tested for association using a Spearman's rank order correlation test to allow for non-linearity.

Morphometric analysis

For scanning electron microscopy (SEM) sponges were cut into 1 mm^3 pieces and fixed in a cocktail consisting of 1% OsO_4, 2% glutaraldehyde in 0.45 mol L^{-1} sodium acetate buffer with 10% sucrose at 4°C for 6-12 h (Harris and Shaw, 1984). Modifications included

addition of 10% ruthenium red to some samples to preserve mucus on the collar filter and adding 4% OsO_4 directly to the sponge tissue before fixation as above, to minimize contraction of canals. Samples were rinsed in distilled water, dehydrated to 70% ethanol and desilicified in 4% hydrofluoric acid (HF) at room temperature (RT) to dissolve spicules. Following desilicification samples were dehydrated to 100% ethanol, fractured in liquid nitrogen and critical point dried. Pieces were mounted on aluminum stubs using an eyebrow brush, gold coated and viewed in a field emission scanning electron microscope (SEM; JEOL 6301 F). Some pieces of *C. delitrix* and *C. vaginalis* were embedded in paraffin wax, sectioned at 12 or 30 μm and mounted on aluminum stubs. Prior to embedding *C. delitrix* (which bores into coral and so is surrounded by the coral skeleton) was placed in 5% ethylenediamenetetracetic acid (EDTA) for 24 hr to remove the coral skeleton. After sectioning the wax was removed in toluene for 15 minutes, the stubs were gold coated and viewed in a field emission SEM.

For histology $1cm^3$ pieces of sponge were fixed in 4% paraformaldehyde in filtered seawater for 24 h, rinsed twice in phosphate buffered saline (PBS), dehydrated to 70% ethanol and desilicified in 4% HF/70% ethanol at RT for 24-72 h. *C. delitrix* was decalcified in Cal-Ex Decalcifier (Fisher Scientific) for 24 h. Tissue was embedded in paraffin wax and sectioned at 5 μm (*T. californiana*), 12 μm (*H. mollis* and *C. delitrix*) and 30 μm (*N. problematica* and *C. vaginalis*) and sections stained in Masson's trichrome stain. Images were captured with a QiCam using Northern Eclipse v.7 (Empix Imaging Inc., Mississauga, ON, Canada) on a Zeiss Axioskop2 Plus microscope.

To determine resistance through the aquiferous system, dimensions of the canals and flagellated chambers were measured from both SEM and histological sections using ImageJ (v. 1.43r; NIH). Care was taken to select regions of the canal system that were not contracted by looking at the tissue surrounding the canal system. It was not always possible to identify incurrent vs. excurrent canals; in these instances it was assumed that the dimensions and path length were the same between excurrent and incurrent canals following Riisgård et al. (1993).

The cross-sectional area of each region of the aquiferous system was calculated for a 100 mm^3 (100 μl) piece after Reiswig (1975a) and Leys et al. (2011). Due to differences in the shape of the sponge body, the dimensions for this 100 μl piece differed for each species. For *N. problematica, H. mollis, T. californiana* and *C. delitrix* the inhalant surface was 4.5 x 4.5 mm^2 and the wall 5 mm thick. The body wall of *C. vaginalis* was only 3 mm thick and

therefore a larger inhalant surface was used (5.77 x 5.77 mm^2) to generate the same 100 µl volume for the piece.

Estimating resistance through the canal system

The cost of filtration can be estimated by the power needed to move water through the sponge aquiferous system. The power is estimated by converting oxygen used in filtration to watts of energy. The movement of water experiences friction from the small dimensions of the canal and filter system and this resistance is called the head loss. Therefore, to determine the cost of filtration we calculated the velocity of water through each part of the sponges' aquiferous system, and then estimated the resistance (head loss) at each part of the aquiferous system.

The velocity of water through each region of the aquiferous canal system, u_i, was calculated using the estimated cross-sectional areas for each part of the sponge and known excurrent velocity from the osculum (Reiswig, 1975a):

$$u_i = \frac{u_{ex}A_{osc}}{A_i} \quad (1)$$

where A_i is the cross sectional area of the region, A_{osc} is the cross sectional area of the osculum, and u_{ex} is the measured excurrent velocity from the osculum.

Two separate approaches were used to estimate the resistance through the canal system of sponges. The first uses an approach summarized by Riisgård and Larsen (1995) where a different equation to model each region of the canal system is applied based on the characteristics of the region. The different equations in this first approach reflect the estimated different architectures of different regions of the sponge. The second approach uses only one equation for the whole canal system (Leys et al, 2011), based on the Hagen-Poiseuille equation for fully developed laminar flow in a tube. This approach assumes that different equations do not capture the accurate differences between regions and therefore one equation is more straightforward and just as accurate. A detailed description of the equations is provided in Box 1, Supplementary Information.

Results

Meta-Analysis

Using both dimensions of filter size gathered from electron micrographs and direct volume flow rate measurements resulted in an increase in the estimate of the cost of filtration for species studied previously (polychaetes, sponges, tunicates), in some instances to more than 5 times previously calculated values (Supplementary Information Table S2).

Volume flow rates and oxygen removal

Mean excurrent velocity, volumetric flow rate, and oxygen removal for each species are provided in Table 1. *C. delitrix* had the fastest excurrent velocity; however, *C. vaginalis* had the highest volumetric flow rate (processed the most water) and used the most oxygen. *T. californiana* filtered the smallest volume of water per unit time and removed the least oxygen of all five species.

For all sponge species except *C. delitrix* more oxygen was removed when more water was filtered (Figure 2). For one individual of each species measured over a five minute period, oxygen removal increased with volume filtered except for *C. delitrix* (*N. problematica* Spearman r = 0.813, p<0.0001, *H. mollis* Spearman r = 0.869, p<0.0001; *T. californiana* Spearman r = 0.905, p<0.0001; *C. delitrix* Spearman r = -0.180, p = 0.169; and *C. vaginalis* Spearman r = 0.734, p<0.0001; Figure 2A). Mean oxygen removal between individuals of each species was also positively correlated with the amount of water filtered, again except for *C. delitrix* (Spearman r = 0.843, p < 0.0001; Figure 2B).

Effect of ambient flow on pumping rates

Callyspongia vaginalis responded to changes in ambient flow with changes to both excurrent velocity and oxygen used but the sponge's response depended on the magnitude of ambient current (Figure 3A,B). An increase in ambient flow from 0-5 cm s^{-1} caused a reduction in both excurrent velocity and oxygen removal, but when ambient current rose from 5-15 cm s^{-1}, then excurrent velocity and oxygen removal both increased. At ambient currents greater than 15 cm s^{-1} however, excurrent velocity and oxygen removal did not change (Figure 3B). Overall, both excurrent velocity (Spearman r = 0.141, p<0.001) and oxygen removal (Spearman r = -0.221, p<0.0001) of *C. vaginalis* were not correlated with ambient current (Figure 3A,B). The same is shown by the filtration to respiration (F/R) ratio which

did not change with increasing ambient flow, remaining at about 0.42 ± 0.03 L umol^{-1} O_2 (Spearman r = 0.232, p<0.0001, Figure 3C).

For *Cliona delitrix* excurrent velocity was positively correlated with ambient flow (Spearman r = 0.485, p<0.0001, Figure 4A,B), however the osculum constricted in response to the flow generated by the pump, reducing in area from 4 cm^2 to less than 2 cm^2 (Figure 4A). The reduced osculum size meant excurrent velocity increased but volumetric flow (volume filtered) decreased with more ambient current (Spearman r = -0.407, p<0.0001, Figure 4A,B). Oxygen removal (μmol hr^{-1}) initially increased at ambient velocities of 0-5 cm s^{-1}, but overall oxygen removal was negatively correlated with ambient current (Spearman r = -0.456, p<0.0001, Figure 4A,B). At ambient currents greater than 15 cm s^{-1} the excurrent velocity increased due to the constriction of the osculum, and oxygen removal decreased correspondingly. As with *Callyspongia vaginalis*, in *Cliona delitrix* there was no significant change in filtration to respiration (F/R) ratio with increasing ambient flow (0.40 ± 0.18 L umol^{-1} O_2, Spearman r = 0.307, p<0.0001, Figure 4C).

Estimating the cost of filtration

Dimensions of each region of the aquiferous canal system for the five species of demosponges studied are given in Table 2. The path the water travels is illustrated in Figure 5. Briefly, water flows in through minute holes (ostia) in the dermal membrane (a three layered tissue) into a large subdermal space in four of the five species (except possibly for *C. delitrix*). From there, water enters into the largest incurrent canals which branch into smaller and smaller canals leading to the choanocyte chambers (Supplemental Information Figure S3). *Callyspongia vaginalis* is distinct from the other species in that the smallest incurrent canals empty into a common lacunar space that holds the choanocyte chambers as described by Johnston and Hildemann (1982) (Figure 6A). For *C. vaginalis* therefore, openings between the choanocytes were considered the equivalent of prosopyles (Figure 6B). In the other four species, water enters the choanocyte chambers from the smallest incurrent canal through one or more prosopyles. At choanocyte chambers water moves through the collar microvilli. In *H. mollis* a set of cells forms a flat layer between all collars in the chamber (Figure 6C). In both *N. problematica* and *C. vaginalis* a dense mesh of glycocalyx occurs in the same region between each of the collars (Figure 6B,D). Although a similar gasket has not been found yet in *T. californiana* and *C. delitrix* (Figure 6E,F), this sort of structure may be more common in demosponges than has previously been appreciated since those made from mucus glycocalyx are difficult to preserve. A glycocalyx mesh was found between the

microvilli of the choanocyte cells in each species studied (Figure 6B), but in the case of *T. californiana* and *C. delitrix* it was only found in a few well-preserved choanocytes within a chamber. After passing through the glycocalyx mesh filter on the collar, the water flows into the chamber and from there out of the apopyle (exit of the sponge choanocyte chamber). In *T. californiana*, the apopyle consists of a sieve-plate (Figure 6E); in other sponges it is a circular aperture. From the apopyle the water enters small excurrent canals that merge into increasingly larger canals before flowing out of the osculum.

Cross-sectional area, velocity of water and head loss for each region of the canal system calculated using the models of Riisgård and Larsen (1995) and Leys et al. (2011) are given in Table 3. In each species the cross-sectional area increases as the water enters the choanocyte chambers (Table 3; Figure 7). Velocity through each region (u_i) was calculated from total cross-sectional area of each region (i), A_i, and excurrent (ex) velocity out of the sponge osculum, u_{ex}, using Equation 1. The effective velocity u_i through the collar slit of the two warm-water species *C. vaginalis* and *C. delitrix*, was 0.018 mm s^{-1} and 0.017 mm s^{-1} respectively, which is 2-10 times higher than the effective velocity in the temperate species (*N. problematica* = 0.009 mm s^{-1}, *H. mollis* = 0.006 mm s^{-1}, and *T. californiana* = 0.002 mm s^{-1}), a difference arising from the higher excurrent velocities of *C. delitrix and C. vaginalis*. The total head loss through the canal system – the sum of head loss through each region – is also 5-17 times higher for the tropical species (Table 3).

To determine the cost of filtration, the power required to pump water across the sponge, P_p, was calculated using the total head loss, ΔH, and volume flow rate, Q, and divided by the total measured oxygen removal R_{tot} (Riisgård and Larsen, 1995) using the conversion 1 μL O_2 hr^{-1} = 5.333 μW (Riisgård, 1988) and the mean oxygen removal and volume flow rates reported in Table 1. Using the model by Riisgård and Larsen (1995) the estimates of the cost of filtration were quite variable, ranging from 1% for *T. californiana* to 15% for *C. delitrix.* The simplified model developed by Leys et al. (2011) gives the same relationship for cost of filtration between the five species of demosponge, although the range is slightly lower at 1-12% for *T. californiana* and *C. delitrix* respectively. Both models estimate a very similar cost of pumping for each species. Both of the warm water species *C. vaginalis* and *C. delitrix* had the highest cost of pumping regardless of the model used (Table 3).

Discussion

Our study aimed to assess the energetic cost of filtration in demosponges and to determine whether sponges reduce their cost of filtration by taking advantage of ambient currents. Of the five species of demosponges studied, the tropical species *Cliona delitrix* and *Callyspongia vaginalis* filtered the most water and extracted the most oxygen per gram of tissue. Because volumetric flow rate drives the model describing the energy required to overcome the resistance through the sponge aquiferous system, both tropical sponges have higher estimates of the cost of filtration than the three temperate demosponges *Neopetrosia problematica, Haliclona mollis,* and *Tethya californiana*. Our data also show that the filtration/respiration (F/R) ratio is constant for ambient flow velocity and therefore the cost of filtration depends only on the amount of water filtered. This suggests that the cost of filtration for demosponges varies by species and that reducing the volume of water filtered would reduce the cost of filtration in regions and seasons with lower food availability.

Interestingly, we found that demosponges can control the water flow through their bodies by responding behaviourally to changes in ambient flow. Both *C. delitrix* and *C. vaginalis* reduce the amount of water filtered at very high ambient velocities, which may be a mechanism to protect themselves from damage during storms. This reduction in the amount of water filtered at very high ambient velocities also suggests that neither species uses current induced flow, despite the cost of filtration being higher than previously estimated.

The cost of pumping

Animals allocate energy to a variety of processes including growth, reproduction, feeding, and digestion. For filter feeders, the energy allocated to feeding has been considered to be low, at 0.1 – 4% of total metabolism based on theoretical models (Jørgensen, 1955; Jørgensen et al., 1986; Jørgensen et al., 1988; Riisgård et al., 1993; Riisgård, 1988 ; Riisgård, 1989). In those studies the cost of filtration was assumed to be equivalent to the energy lost due to frictional resistance as water flows through the filter and canals. By changing filter size and volume flow rate using numbers gleaned from the literature, the estimate for the cost of filtration increased by up to 5 times previous estimates. This suggests that both filter dimensions and volume flow rates contribute substantially to the cost of pumping in filter feeding invertebrates. It also suggests that accurate measurements of filter dimensions and volume flow rates are important when modeling the cost of filtration and focused our attention on these for this study.

Although there were differences in gross morphology among the five species of sponge we studied, we found similar morphologies of the filter for each of the species studied. The cost of pumping was variable ranging from 1% (*T. californiana*) to 12-15% (*C. delitrix*) of the total oxygen consumed, assuming oxygen consumed is used for all metabolism including filtration. Previous estimates on the energetic cost of pumping in demosponges also show a large range, from 0.4% for *Haliclona urceolus* (Riisgård et al., 1993) to 25% for *Neogombata magnifica* (Hadas et al., 2008). Although this variability may reflect the use of theoretical models (Riisgård et al. 1993) compared to direct measurements (Hadas et al. 2008), our results suggest that the main variability in 'cost' arises from differences in the volume of water processed.

Whether a single equation was used for all structures of the aquiferous system (Leys et al. 2011) or different equations were used to describe potentially different aspects (aperture, duct, channel, and lattice network openings) of the passages (Riisgård and Larsen 1995), the estimate of cost was very similar. Small differences in cost found between the two models reflect differences in the dimensions and the velocity of water at the aperture or structure. The greatest head loss occurred at the glycocalyx mesh filter, which had the smallest dimensions and therefore offered the greatest resistance (Supplemental Information Table S2). And yet while the mesh size was smaller in *T. californiana* than *C. delitrix* the head loss was far greater across the collar filter of *C. delitrix* because the velocity of water at its filter was substantially higher. Velocity at each aperture was governed by the exit velocity of each species, and so the two tropical species, having the largest volumetric flow rates (processing the most water), had the highest cost of filtration (Table 3). In addition, when individuals of each species filtered more water they also consumed more oxygen (Figure 2), demonstrating that the energetic cost of pumping depends on how much water is being pumped at any one time. This implies that sponges could save energy in times of low food availability by reducing the volume of water filtered.

That filtering more water costs more energy is not necessarily intuitive because sponges could easily use ambient flow to enhance the movement of water through their canal system. Our data demonstrate that neither *C. delitrix* nor *C. vaginalis* uses higher ambient flow to reduce the cost of filtration. Instead both sponges actively modify their behaviour to increase or reduce the volume filtered. How a sponge changes its pumping rate and volume filtered however, is not known. One mechanism might be to increase the rate of flagellar beat in the choanocyte chambers or activate more pumping units. This would increase the velocity of water through the canal system and therefore increase the volume of water filtered.

Dilation of the canals including the osculum diameter might also occur in addition to the increase in flagellar beat, which would increase the volume of water filtered. According to the Hagen-Poiseuille equation for flow through a pipe, the energy required to move water through a pipe is proportional to the square of the flow rate, therefore the more water actively pumped through the canal system at any one time would increase the resistance and therefore also the energetic cost of pumping. Similarly, since head loss is inversely proportional to the canal diameter to the power of four then constriction of the canals would result in reduced volume flow rate and increased head loss. Sponges likely control the rate of flagellar beating to save energy when the sponge contracts. We did not look at the energy spent on the flagellar beating nor the drag on the flagellum when estimating the cost of pumping, which is a limitation in the model and probably makes our estimates more conservative.

It is important to consider why the two tropical species of demosponge had higher volume flow rates and therefore higher estimates for the cost of filtration in this study. Differences in pumping rates between species can be caused by structural differences in the sponge canal system (Reiswig, 1975a), microbial content (Weisz et al., 2008), and tissue density (Turon et al., 1997). In addition, Riisgård et al. (1993) found that volume flow rate in *Haliclona urceolus* increased up to ten times with a change in temperature from 6°C to 15°C. The higher volume flow rate per gram weight in the two tropical species in this study therefore may be a result of the higher temperature of water and lower viscosity. However, due to the high energetic cost of filtering more water it would only be adaptive to have such high volume flow rates if there is enough food available – either as picoplankton to be filtered from the water or from endosymbionts – to support the high energetic needs. We did not measure carbon flux in these species but this is a planned next step.

Sponges are found in almost every marine and freshwater habitat and, with the exception of carnivorous sponges, all feed on ultraplankton and dissolved organic carbon. Increasing cross-sectional area through the canal system slows the velocity of water, enabling food capture either in the small incurrent canals or at the filter. Slight differences in filtration ability and size of plankton captured between different species of sponges are known (Reiswig, 1975b; Turon et al., 1997; Yahel et al., 2007). There is little information, however, on the relationship between filtration ability, diet, and microarchitecture of the aquiferous canal system. Among the five species studied here, slight variations in the architecture of the aquiferous canal system were found such as the lacunar space in *C. vaginalis* and the sieve-plate apopyle of *T. californiana*. We also found wide differences in the velocities of water

measured out of the osculum, although similar velocities of water at the filter (Table 4). This suggests that despite wide differences in volume flow rates and adaptations to a variety of habitats and ecological niches, the canal system of sponges is designed to slow the velocity of water down to a certain speed that enables food capture at the filter. The small differences that were found in both velocities at the filter and filter dimensions may reflect small differences in preferred plankton size or filtration ability. A smaller mesh size may allow the sponge to capture smaller food particles, but due to the higher cost of filtration may also restrict the volume of water processed. Our model predicted that both tropical species *C. vaginalis* and *C. delitrix* had faster velocities of water at the collar filter. *C. vaginalis* lacks the small incurrent canals leading into the choanocyte chambers, suggesting that it does not rely on pinacocyte capture of plankton in the canals.

Ambient currents do not enhance excurrent velocity

One way to reduce the cost of pumping in sponges would be to take advantage of ambient currents by using passive flow. In both *C. delitrix* and *C. vaginalis* excurrent volume flow rates were not correlated to the ambient currents, suggesting they do not use passive flow. Rather, both species decreased their volume flow rate when ambient velocities reached a certain level, which may be to reduce damage caused by high currents or resuspension of sediments during storms (Bannister et al., 2012; Gerrodette and Flechsig, 1979; Tompkins-MacDonald and Leys, 2008).

We suggest that the discrepancy in our results and those of Vogel who first described the apparent use of induced current by sponges (Vogel, 1974; Vogel, 1977) are due to the use of excurrent velocity rather than volume flow rate and the use of individual points in time rather than a full time series. The increased excurrent velocity recorded by Vogel (1977) in the species *Amphimedon viridis* (referred to as *Haliclona viridis*), *Ircinia variabilis* (referred to as *Ircinia fasciculata*), and *Aplysina fistularis* (referred to as *Verongia fistularis*), may have been behavioural responses, as shown here in *C. delitrix* in which contraction of the osculum caused increased excurrent (exit) velocity, but reduced volumetric flow rate as ambient currents increased. A full time series with measurements of the osculum diameter throughout would indicate whether Vogel's findings were actually a result of current induced flow or rather a behavioural response to the increased current.

Other sponges have also been reported to show reduced excurrent flow with increased ambient flow. Savarese et al. (1997) noted that two individuals of the globose freshwater sponge *Baikalospongia bacillifera* in Lake Baikal monitored over a diel cycle showed

negative correlations between ambient and excurrent flow rates. In addition, they noted periodic cessation of pumping on the order of minutes to hours that did not correlate with ambient flow. Reiswig (1971) also found periodic oscular closures and therefore cessations of pumping with *Tethya crypta* that were negatively correlated to wave action. Here, we found both *C. vaginalis* and *C. delitrix* reduced the volume of water filtered when ambient currents reached a certain threshold. Some demosponges therefore show a large amount of control of filtration despite fluctuations in the ambient water velocity.

General conclusions

The over-arching finding of this work is that the energetic costs of sponge pumping are closely coupled to volumetric flow (how much water is filtered). We found a considerable variation in flow rates and corresponding costs, with tropical sponges having higher volumetric flow rates and costs. The difference may be related to food availability and temperature. We also found that despite the variation in costs, the similarity in architecture and design of the aquiferous canal system is such that the velocity of water slows at the filter, although each species accomplishes this in slightly different ways, thus making them all well suited to feed on ultraplankton and dissolved organic carbon.

For the three temperate demosponges, our estimates for the cost of pumping are comparable to those found by Riisgård et al. (1993) for what he termed the 'standard sponge'. However, the two tropical demosponges we studied had much higher volume flow rates with much higher cost of pumping; the cost of pumping for *C. delitrix* was more comparable to the cost of pumping for other sponges found by both Leys et al. (2011) and Hadas et al. (2008). It is likely that habitat and ecological niche of sponges has led to adaptations in body form and physiology over time and together these play a large role in differences in cost of pumping. Our third main finding was that despite the higher costs for the two tropical sponges ambient flow is not a positive driver of flow through the sponge and is therefore not used to reduce the cost of filtration. Instead both of these sponges responded to increased ambient currents by reducing the volume filtered. In the shallow sandy habitat of both *C. delitrix* and *C. vaginalis* increased ambient flow results in resuspension of particles. Demosponges have sensory cilia in their osculum, which allow them to sense and respond to changes in their environment (Ludeman et al., 2014). Reiswig (1975a) showed that several species of tropical demosponge responded to storm events by reducing filtration, and so it is likely that the demosponges we studied here respond to changes in ambient currents to reduce damage to their filter that would be caused by intake of sediments resuspended during high ambient currents.

Acknowledgements:

We thank the directors and staff at the Bamfield Marine Sciences Center, Bamfield, British Columbia and the Smithsonian Tropical Research Station, Bocas, Panama, for use of facilities and N. Lauzon and N. Trieu for assistance with field work and histology respectively and A. Kahn and G. Yahel for valuable comments on an earlier version. Data for this study is accessible at the University of Alberta Education Resource Archive (ERA).

Competing Interests:

No competing interests declared.

Author Contributions:

DAL, SPL, and MR conceived the experiments; SPL collected the sponges; DAL, SPL, and MR performed the experiments; DAL carried out the electron microscopy, histology, statistical analysis and morphometric model; DAL and SPL wrote the paper.

Funding:

DAL acknowledges a Nortek student equipment grant for use of a Vectrino Profiler for portions of this work, and the Company of Biologists for a Travelling Fellowship to carry out the work in Panama. Funding for this work came from the Natural Sciences and Engineering Research Council of Canada (NSERC) through a Discovery Grant to SPL and National Science Foundation (NSF) CAREER Grant (NSF-OCE 1151314) to MAR.

References

Bannister, R. J., Battershill, C. N. and de Nys, R. (2012). Suspended sediment grain size and mineralogy across the continental shelf of the Great Barrier Reef: Impacts on the physiology of a coral reef sponge. *Continental Shelf Research* **32**, 86-95.

Best, B. (1988). Passive suspension feeding in a sea pen: effects of ambient flow on volume flow rate and filtering efficiency. *The Biological Bulletin* **175**, 332-342.

Bidder, G. P. (1923). The relation of the form of a sponge to its currents. *Quarterly Journal of Microscopical Science* **67**, 293-323.

Denny, M. (1993). Air and water: the biology and physics of life's media. Princeton, N.J: Princeton University Press.

Genin, A., Karp, L. and Miroz, A. (1994). Effects of flow on competitive superiority in scleractinian corals. *Limnology and Oceanography* **39**, 913-924.

Gerrodette, T. and Flechsig, A. O. (1979). Sediment-induced reduction in the pumping rate of the tropical sponge *Verongia lacunosa*. *Marine Biology* **55**, 103-110.

Gili, J. M. and Coma, R. (1998). Benthic suspension feeders: their paramount role in littoral marine food webs. *Trends in Ecology and Evolution* **13**, 316-321.

Griffiths, C. L. and King, J. A. (1979). Energy expended on growth and gonad output in the ribbed mussel *Aulacomya ater*. *Marine Biology* **53**, 217-222.

Hadas, E., Ilan, M. and Shpigel, M. (2008). Oxygen consumption by a coral reef sponge. *Journal of Experimental Biology* **211**, 2185-2190.

Harris, P. and Shaw, G. (1984). Intermediate filaments, microtubules and microfilaments in epidermis of sea urchin tube foot. *Cell and Tissue Research* **236**, 27-33.

Jørgensen, C. (1955). Quantitative aspects of filter feeding in invertebrates. *Biological reviews and biological proceedings of the cambridge philosophical society.* **30**, 391-454.

Jørgensen, C. (1975). Comparative physiology of suspension feeding. *Annual review of physiology* **37**, 57-79.

Jørgensen, C. B. (1966). Biology of suspension feeding. London: Pergamon Press.

Jørgensen, C. B., Famme, O., Kristensen, H. S., Larsen, P. S., Møhlenberg, F. and Riisgård, H. U. (1986). The bivalve pump. *Marine Ecology Progress Series* **34**, 69-77.

Jørgensen, C. B., Larsen, P. S., Møhlenberg, F. and Riisgård, H. U. (1988). The mussel pump: properties and modelling. *Marine Ecology Progress Series* **45**, 205-218.

Knott, N. A., Davis, A. R. and Buttemer, W. A. (2004). Passive flow through an unstalked intertidal ascidian: orientation and morphology enhance suspension feeding in *Pyura stolonifera*. *Biological Bulletin* **207**, 217-224.

LaBarbera, M. (1977). 1. Theory, laboratory behavior, and field orientations. *Paleobiology* **3**, 270-287.

Leys, S., Yahel, G., Reidenbach, M., Tunnicliffe, V., Shavit, U. and Reiswig, H. (2011). The sponge pump: the role of current induced flow in the design of the sponge body plan. *Public Library of Science One* **6 (12)**, e27787.

Ludeman, D., Farrar, N., Riesgo, A., Paps, J. and Leys, S. (2014). Evolutionary origins of sensation in metazoans: functional evidence for a new sensory organ in sponges. *BMC Evol Biol* **14**, 3.

Murdock, G. R. and Vogel, S. (1978). Hydrodynamic induction of water flow through a keyhole limpet (gastropoda, fissurellidae). *Comparative Biochemistry and Physiology Part A: Physiology* **61**, 227-231.

Newell, R. and Branch, G. (1980). The influence of temperature on the maintenance of metabolic energy balance in marine invertebrates. *Advances in Marine Biology* **17**, 329-396.

Reiswig, H. M. (1971). *In situ* pumping activities of tropical demospongiae. *Marine Biology* **9**, 38-50.

Reiswig, H. M. (1975a). The aquiferous systems of three marine demospongiae. *Journal of Morphology* **145**, 493-502.

Reiswig, H. M. (1975b). Bacteria as food for temperate-water marine sponges. *Canadian Journal of Zoology* **53**, 582-589.

Riisgård, H. and Larsen, P. (1995). Filter-feeding in marine macro-invertebrates: pump characteristics, modelling and energy cost. *Biological Reviews* **70**, 67-106.

Riisgård, H., Thomassen, S., Jakobsen, H., Weeks, J. and Larsen, P. (1993). Suspension feeding in marine sponges *Halichondria panicea* and *Haliclona urceolus*: effects of temperature on filtration rate and energy cost of pumping. *Marine Ecology Progress Series* **96**, 177-188.

Riisgård, H. U. (1988). The ascidian pump: properties and energy-cost. *Marine Ecology Progress Series* **47**, 129-134.

Riisgård, H. U. (1989). Properties and energy cost of the muscular piston pump in the suspension feeding polychate *Chaetopterus variopedatus*. *Marine Ecology Progress Series* **56** 157-168.

Riisgård, H. U. and Larsen, P. S. (2001). Minireview: ciliary filter feeding and bio-fluid mechanics - present understanding and unsolved problems. *Limnology and Oceanography* **46**, 882-891.

Savarese, M., Patterson, M. R., Chernykh, V. I. and Fialkov, V. A. (1997). Trophic effects of sponge feeding within Lake Baikal's littoral zone. 1. *In situ* pumping rates. *Limnology and Oceanography* **42**, 171-178.

Shiino, Y. (2010). Passive feeding in spiriferide brachiopods: an experimental approach using models of Devonian Paraspirifer and Cyrtospirifer. *Lethaia* **43**, 223-231.

Thompson, R. J. and Bayne, B. L. (1972). Active metabolism associated with feeding in the mussel *Mytilus edulis* L. *Journal of Experimental Marine Biology and Ecology* **9**, 111-124.

Tompkins-MacDonald, G. J. and Leys, S. P. (2008). Glass sponges arrest pumping in response to sediment: implications for the physiology of the hexactinellid conduction system *Marine Biology* **154**, 973-984.

Trager, G. C., Hwang, J.-S. and Strickler, J. R. (1990). Barnacle suspension-feeding in variable flow. *Marine Biology* **105**, 117-127.

Turon, X., Galera, J. and Uriz, M. J. (1997). Clearance rates and aquiferous systems in two sponges with contrasting life-history strategies. *Journal of Experimental Zoology* **278**, 22-36.

Vogel, S. (1974). Current-induced flow through the sponge *Halichondria*. *Biological Bulletin* **147**, 443-456.

Vogel, S. (1977). Current-induced flow through living sponges in nature. *Proceedings of the National Academy of Science USA* **74**, 2069-2071.

von Dassow, M. (2005). Flow and conduit formation in the external fluid-transport system of a suspension feeder. *J Exp Biol* **208**, 2931-2938.

Weisz, J., Lindquist, N. and Martens, C. (2008). Do associated microbial abundances impact marine demosponge pumping rates and tissue densities? *Oecologia* **155**, 367-376.

Yahel, G., Marie, D. and Genin, A. (2005). InEx—a direct in situ method to measure filtration rates, nutrition, and metabolism of active suspension feeders. *Limnology and Oceanography: Methods* **3**, 46-58.

Yahel, G., Whitney, F., Reiswig, H. M., Eerkes-Medrano, D. I. and Leys, S. P. (2007). In situ feeding and metabolism of glass sponges (Hexactinellida, Porifera) studied in a deep temperate fjord with a remotely operated submersible. *Limnology and Oceanography* **52**, 428-440.

Young, C. and Braithwaite, L. (1980). Orientation and current-induced flow in the stalked ascidian *Styela montereyensis*. *The Biological Bulletin* **159**, 428-440.

Table 1| Mean excurrent velocity, volume flow rate, and oxygen removal from five species of demosponges. Mean ± SD. Both volume flow rate and oxygen removal are standardised by sponge volume (per mL sponge) and sponge weight (per gram dry weight, gDW).

Species	n	Excurrent Velocity (cm s^{-1})	Volume Flow Rate (L h^{-1})	Volume Flow Rate (L h^{-1} mL^{-1} sponge)	Volume Flow Rate (L $h^{-1}$$gDW^{-1}$ sponge)	Oxygen removal (µmol L^{-1})	Oxygen removal (µmol h^{-1} mL^{-1} sponge)	Oxygen removal (µmol h^{-1} gDW^{-1} sponge)
Cliona delitrix	8	11.04 ± 0.54	175.04 ± 38.83	0.39 ± 0.02	4.33 ± 0.21	2.20 ± 1.04	0.83 ± 0.38	9.32 ± 4.29
Callyspongia vaginalis	10	5.93 ± 0.67	44.49 ± 7.29	1.13 ± 0.18	18.02 ± 2.95	2.63 ±0.53	3.12 ± 0.99	49.72 ± 15.87
Tethya californiana	9	1.95 ± 0.30	5.16 ± 0.73	0.09 ± 0.007	0.28 ± 0.02	2.71 ± 0.60	0.23 ± 0.04	0.71 ± 0.12
Haliclona mollis	10	3.04 ± 0.30	2.92 ± 0.47	0.13 ± 0.01	1.08 ± 0.11	2.32 ± 0.53	0.31 ± 0.08	2.53 ± 0.63
Neopetrosia problematica	6	1.37 ± 0.25	0.53 ± 0.11	0.28 ± 0.05	2.26 ± 0.41	1.35 ± 0.14	0.38 ± 0.07	3.08 ± 0.63

Table 2| Dimensions of the aquiferous canal system in sponges

Numbers represent means of 3-75 measurements taken from 1-6 images from either scanning electron microscopy (SEM) or histology and light micrographs. Dimensions of collar slit, including the glycocalyx mesh on the collar, are in bold representing the filtration apparatus.

	Haliclona permollis*		***Aphrocallistes vastus****		***Neopetrosia problematica***		***Haliclona mollis***		***Tethya californiana***		***Callyspongia vaginalis***		***Cliona delitrix***	
Region of the aquiferous canal system	Diameter (μm)	Path length (μm)	Diameter (μm)	Path length (μm)	Diameter (μm)	Path length (μm)	Diameter (μm)	Path length (μm)	Diameter (μm)	Path length (μm)	Diameter (μm)	Path length (μm)	Diameter (μm)	Path length (μm)
Ostia	20.6		3.89	0.50	24.5	0.5	14.3	0.5	40.6	0.5	31.2	0.5	37.3	0.5
Subdermal space			90	82	242	86.1	95.0	50.6	177	105	168	131		
Large incurrent canal	50-340	3000	366	2000	383	2944	333	930	678	1118	407	923	294	1130
Medium incurrent canal				529	156	648	140	834	170	1118	195	725	144	969
Small incurrent canal				237	33	250	51.3	151.9	34.7	68.9	43.8	1	60.1	251
Prosopyles	1 to 5		2.15		3.60	0.5	2.37	0.5	4.52	0.5	1.61	0.5	2.59	0.5
Pre-collar space			2	2	1.3	2.6	5.7	3.6	1.6	2.2	0.5	2.6	0.69	2.19
Glycocalyx mesh			**0.045**	**0.010**	**0.095**		**0.166**		**0.059**		**0.052**		**0.118**	
Collar slit	**0.120**	**0.140**	**0.119**	**0.070**	**0.074**	**0.118**	**0.110**	**0.100**	**0.066**	**0.086**	**0.069**	**0.109**	**0.070**	**0.099**
Glycocalyx mesh			**0.045**	**0.010**										
Post-collar space			2	2	2.6	2.1	3.3	3.3	2.2	3.4	2.6	1.6	2.2	2.65
Chamber	30		56	56	23.3	23.3	28.5	28.5	21.1	21.1	19.7	19.7	16.0	16.0
Apopyle	14	1	26.4	2	16.0	0.5	14.1	0.5	0.90	0.5	5.97	0.5	4.23	0.5
Small excurrent canal				118	45.2	173	51.9	189	34.9	74	52.9	0.5	60.1	251
Medium excurrent canal					130	648	155	546	170	994	179	1096	144	969
Large excurrent canal	102-235	3000	405	2840	282	2944	411	930	678	994	339	1342	294	1130
Osculum	2300		44734	279000	3464	6676	5527	7420	8666	2184	16209	198410	22666	9983
Chambers per mm^3	12,000		1,876		9,792		2,684		14,403		14,358		35,175	
Collars per chamber	95		260		80		139		99		93		50	
Microvilli per collar	28		38		40		40		39		33		33	

*from Reiswig 1975a and **Leys et al. 2011

Table 3| Morphometric model of the aquiferous system in five species of demosponges. Estimated total cross-sectional area for each region from the dimensions listed in Table 2. The velocity of water flow through each area u_∞ was calculated from cross-sectional area A_i and measured excurrent velocity u_{ex} out of the osculum using equation (4). Head loss H in each region was calculated using equations (3-6) from dimensions and velocity u_∞ of each region. Riisgård and Larson's (1995) model used a different equation of head loss for each region of the aquiferous canal system, whereas Leys et al. (2011) model used only equation (3). The sum of the head loss ΔH and measured volume flow rate are used to calculated the pumping power P_p using equation (2). The cost of pumping η (%) is then estimated using equation (1) from the pumping power P_p and the measured respiration rate R_{tot}. The collar slit is in bold, representing the filtration apparatus.

	Neopetrosia problematica				*Haliclona mollis*				*Tethya californiana*				*Callyspongia vaginalis*				*Cliona delitrix*			
			Head loss, H (µm H_20)				Head loss, H (µm H_20)				Head loss, H (µm H_20)				Head loss, H (µm H_20)				Head loss, H (µm H_20)	
Region of the aquiferous canal system	Cross-sectional area, A_i (mm^2)	Velocity, u_i (mm/s)	Riisgård and Larson (1995)	Leys *et al* (2011)	Cross-sectional area, A_i (mm^2)	Velocity, u_i (mm/s)	Riisgård and Larson (1995)	Leys *et al* (2011)	Cross-sectional area, A_i (mm^2)	Velocity, u_i (mm/s)	Riisgård and Larson (1995)	Leys *et al* (2011)	Cross-sectional area, A_i (mm^2)	Velocity, u_i (mm/s)	Riisgård and Larson (1995)	Leys *et al* (2011)	Cross-sectional area, A_i (mm^2)	Velocity, u_i (mm/s)	Riisgård and Larson (1995)	Leys *et al* (2011)
Ostia	3.37	1.04	111	4	0.90	3.90	709	42	1.38	1.76	113	2	12.8	0.68	51	1	2.82	6.57	409	9
Subdermal space	19.7	0.18	56	7	22.2	0.16	239	96	16.7	0.14	46	26	21.8	0.40	10	12				
Large incurrent canal	15.9	0.22	16	16	14.4	0.24	6	6	21.7	0.11	2	2	14.1	0.62	9	9	3.31	5.60	338	338
Medium incurrent canal	7.21	0.49	26	26	3.21	1.09	45	45	24.8	0.10	19	19	2.70	3.25	47	47	2.57	7.22	1026	1026
Small incurrent canal	5.79	0.61	491	491	4.16	0.84	278	278	3.66	0.66	25	25	3.67	2.39	3	3	1.71	10.84	1969	1969
Prosopyles	494	0.007	438	103	346	0.010	922	330	172	0.014	380	71	55.2	0.159	3434	1806	17.7	1.04	9714	3186
Pre-collar space	255	0.014	49	49	775	0.005	5	5	504	0.005	55	55	170	0.051	6768	6768	264	0.070	19158	19158
Collar slit	**376**	**0.009**	**288**	**797**	**546**	**0.006**	**471**	**73**	**1237**	**0.0020**	**147**	**521**	**492**	**0.018**	**668**	**8202**	**1095**	**0.017**	**2300**	**1969**
Post-collar space	412	0.009	13	13	405	0.009	9	9	1077	0.0022	6	6	566	0.015	17	17	1019	0.018	37	37
Chamber	408	0.009	2	2	171	0.020	1	1	488	0.005	0	0	406	0.022	3	3	674	0.027	4	4
Apopyle	208	0.02	1	0	44.6	0.08	4	0	110	0.02	14	13	40.3	0.22	8	1	52.1	0.36	15	3
Small excurrent canal	4.66	0.75	6	6	6.79	0.52	24	24	2.47	0.98	6	6	0.52	16.9	0	0	1.71	10.84	97	97
Medium excurrent canal	3.47	1.01	128	128	6.33	0.55	52	52	24.8	0.10	149	149	2.87	3.05	2288	2288	2.57	7.22	1985	1985
Large excurrent canal	1.21	2.90	165	165	13.1	0.27	13	13	21.7	0.11	1	1	3.04	2.88	140	140	3.31	5.60	371	371
Osculum	0.26	13.66	10	33	0.12	30.44	47	33	0.11	21.95	25	3	0.15	59.33	179	176	0.17	110.41	622	8
Volume flow rate, *Q* (mL/min)			**9.0**				**48.6**				**82.1**				**742**				**2668**	
Respiration, R_{tot} (µW)			**87**				**790**				**1396**				**14218**				**42102**	
Head loss, ΔH (µm H_20)			**2138**	**2303**			**1881**	**1008**			**826**	**771**			**4066**	**6185**			**14307**	**11304**
Pumping Power, P_p (µW)			**3**	**3**			**15**	**8**			**11**	**11**			**504**	**766**			**6377**	**5038**
Cost of pumping, η (%)			**3.70**	**3.99**			**1.89**	**1.01**			**0.80**	**0.74**			**3.54**	**5.38**			**15.15**	**11.97**

Figures

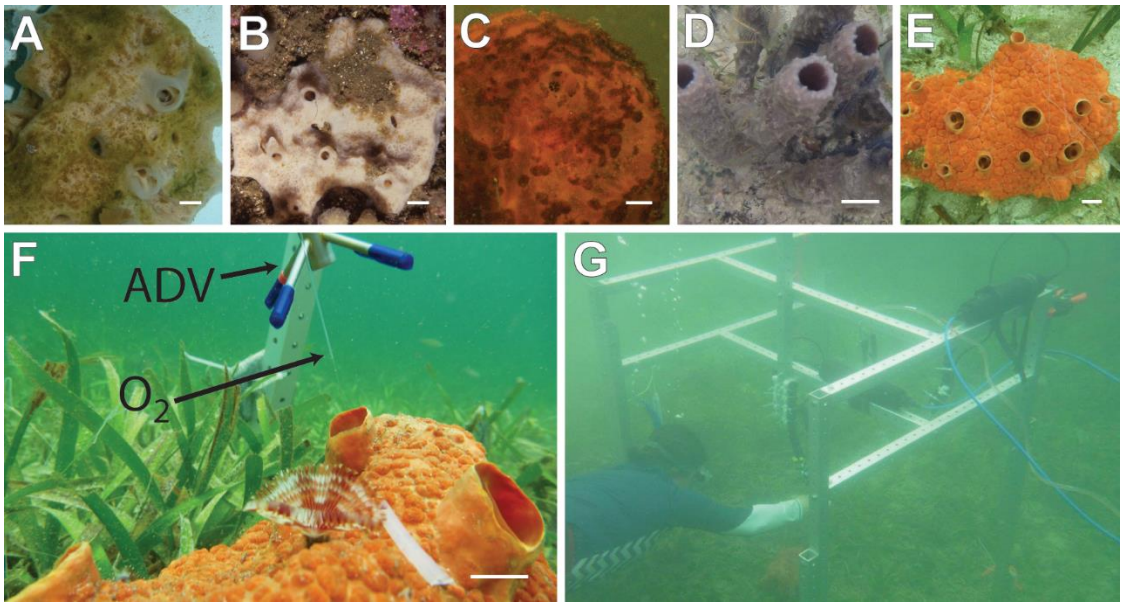

Figure 1| Experimental set-up and species used.

Haliclona mollis (A), *Neopetrosia problematica* (B) and *Tethya californiana* (C) were collected and studied *in vitro* in Bamfield, British Columbia, Canada. *Callyspongia vaginalis* (D) and *Cliona delitrix* (E) were studied *in situ* in Bocas del Toro, Panama. (F) Excurrent velocity was measured out of the osculum using a Nortek Vectrino II acoustic Doppler velocity (ADV) and removal of oxygen was measured using a FirestingO_2 bare fiber sensor (O_2) positioned inside the sponge osculum. (A) Instruments were mounted *in situ* on a frame positioned over the sponge. Scale Bars A,C 0.5 cm; B, 1 cm; D-F, 2 cm.

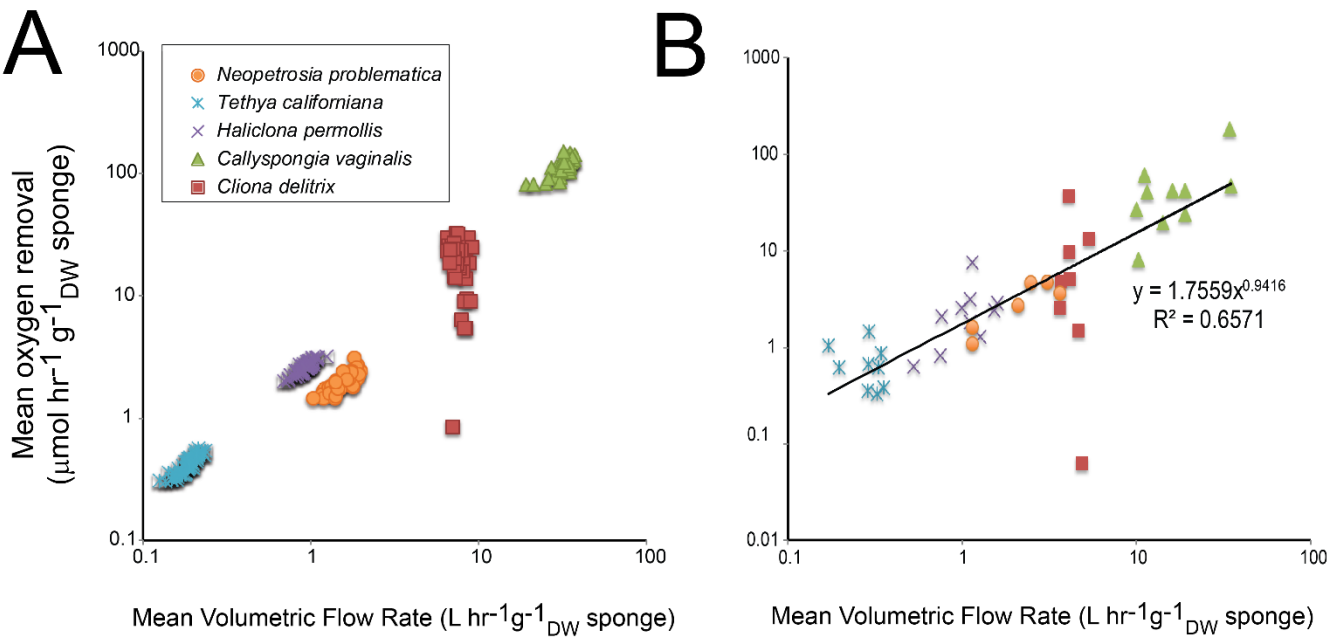

Figure 2| Volumetric flow rates and oxygen removal

(A) Volumetric flow (L hr^{-1} g DW $sponge^{-1}$) and oxygen removal (µmol hr^{-1} g DW $sponge^{-1}$) were recorded for five-minutes and plotted for one individual of each of five species of demosponges. Oxygen removal increased as the volume filtered increased across species, with the exception of *Cliona delitrix* (red). (B) The same trend is seen for oxygen removal and volumetric flow for multiple individuals of each species (*C. vaginalis* N=11; *C. delitrix* N=8; *H. mollis* N=10; *N. problematica* N=7; *T. californiana* N=8).

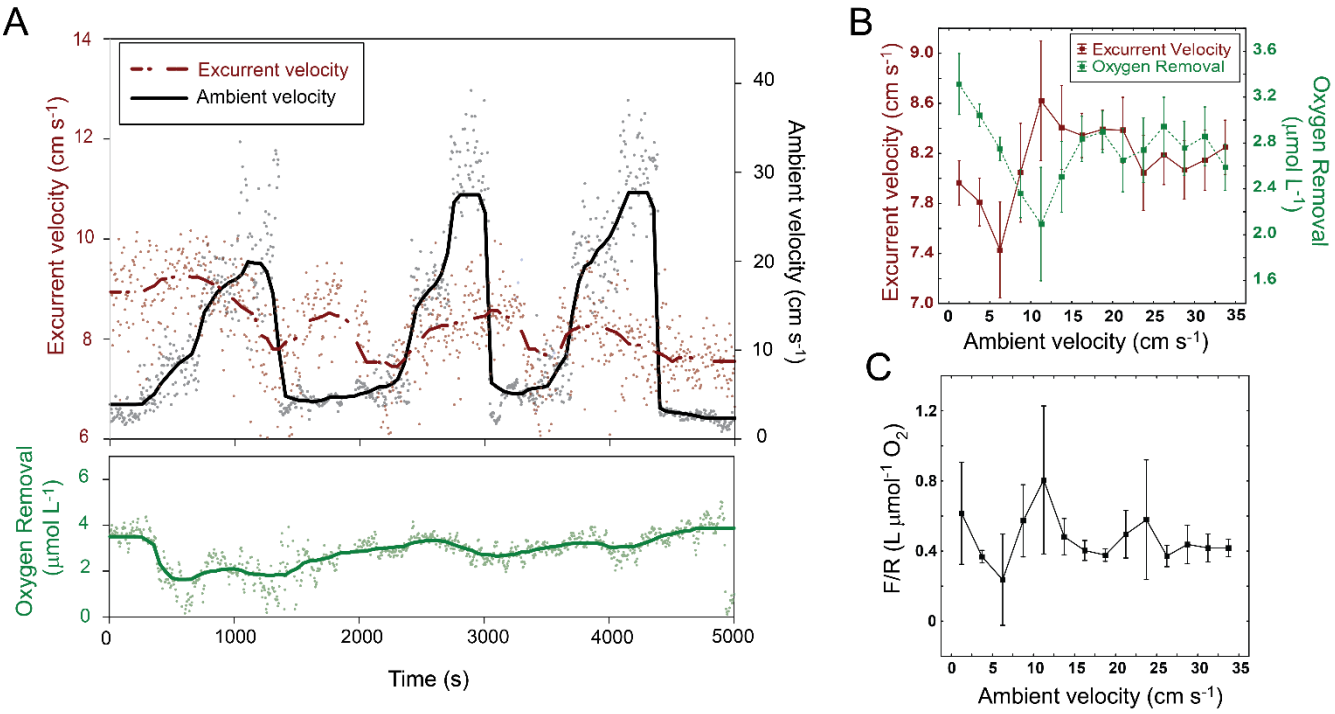

Figure 3| Effect of ambient currents on excurrent velocity and oxygen removal in *Callyspongia vaginalis.* (A) Ambient (black) and excurrent (red) velocity (cm s^{-1}) recorded during an experiment in which ambient velocity was increased every 300 s (5 min) using an underwater aquarium pump over a single sponge. One experiment of three carried out is shown. The sponge responded to each change in ambient velocity, with a general trend of reducing excurrent velocity when ambient current was increased. Oxygen removal also slowly decreased over the course of the experiment. (B) The data in (A) plotted in bins of ambient flow (increments of 2.5 cm s^{-1}) shows that excurrent velocity decreases in response to low ambient currents (0-5 cm s^{-1}) but increases in response to changes in ambient currents of 5-15 cm s^{-1}. Ambient currents greater than 15 cm s^{-1} cause no change in excurrent velocity. Changes in excurrent flow are followed by a change in oxygen removal, with a delay of about 5 cm s^{-1}. There is no correlation between ambient and excurrent velocity (red; Spearman r = 0.141, p <0.001) and ambient velocity and oxygen removal (green; Spearman r = -0.221, p<0.0001). (C) The filtration to respiration (F/R) ration did not change over the course of the experiment (Spearman r = 0.232, p<0.0001)

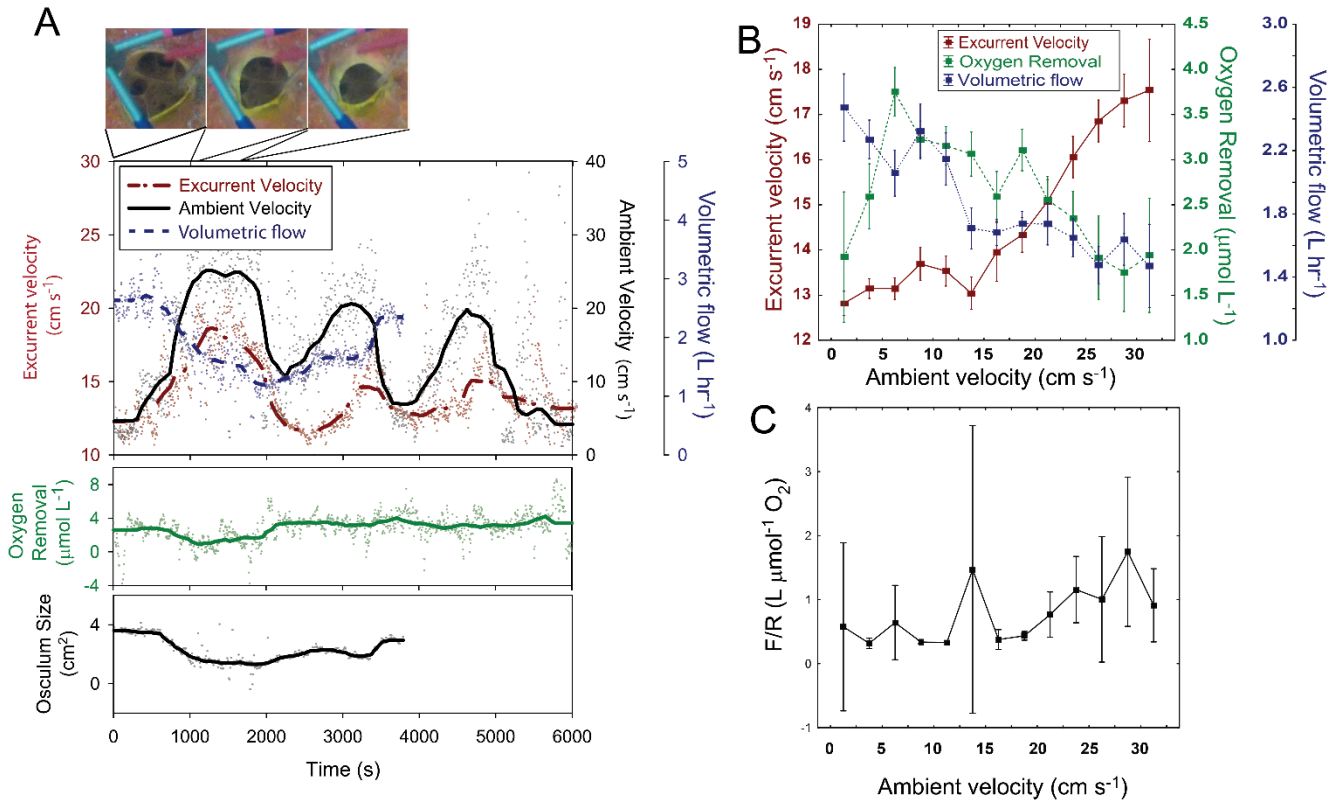

Figure 4| Effect of ambient currents on excurrent flow rate and oxygen removal in *Cliona delitrix*. (A) Ambient (black) velocity was increased every 5 minutes using an underwater aquarium pump over a single sponge. One experiment of three carried out is shown. Excurrent velocity (red) increased with increasing ambient velocity, but contraction of the osculum (top images and lower graph) meant that the volume processed (blue) decreased. Oxygen removal was variable over the course of the experiment. (B) Excurrent velocity binned by ambient flow (in 2.5 cm s^{-1} increments) shows that excurrent velocity increases when ambient flows are greater than 15 cm s^{-1}, and increased excurrent velocity is negatively correlated with oxygen removal. There is a positive correlation between ambient and excurrent velocity (red; Spearman r = 0.485, $p<0.0001$), although a negative correlation between ambient velocity and volume filtered (blue; Spearman r = -0.407, $p<0.0001$). Because the osculum contracts less volume of water is processed, which also corresponds to less oxygen used (green; Spearman r = -456, $p<0.0001$). The initial increase in oxygen removal may be due to the energy required to contract the canals and osculum in response to the ambient current. (C) The filtration to respiration (F/R) ration did not change with different ambient current velocities (Spearman r = 0.307, $p<0.0001$).

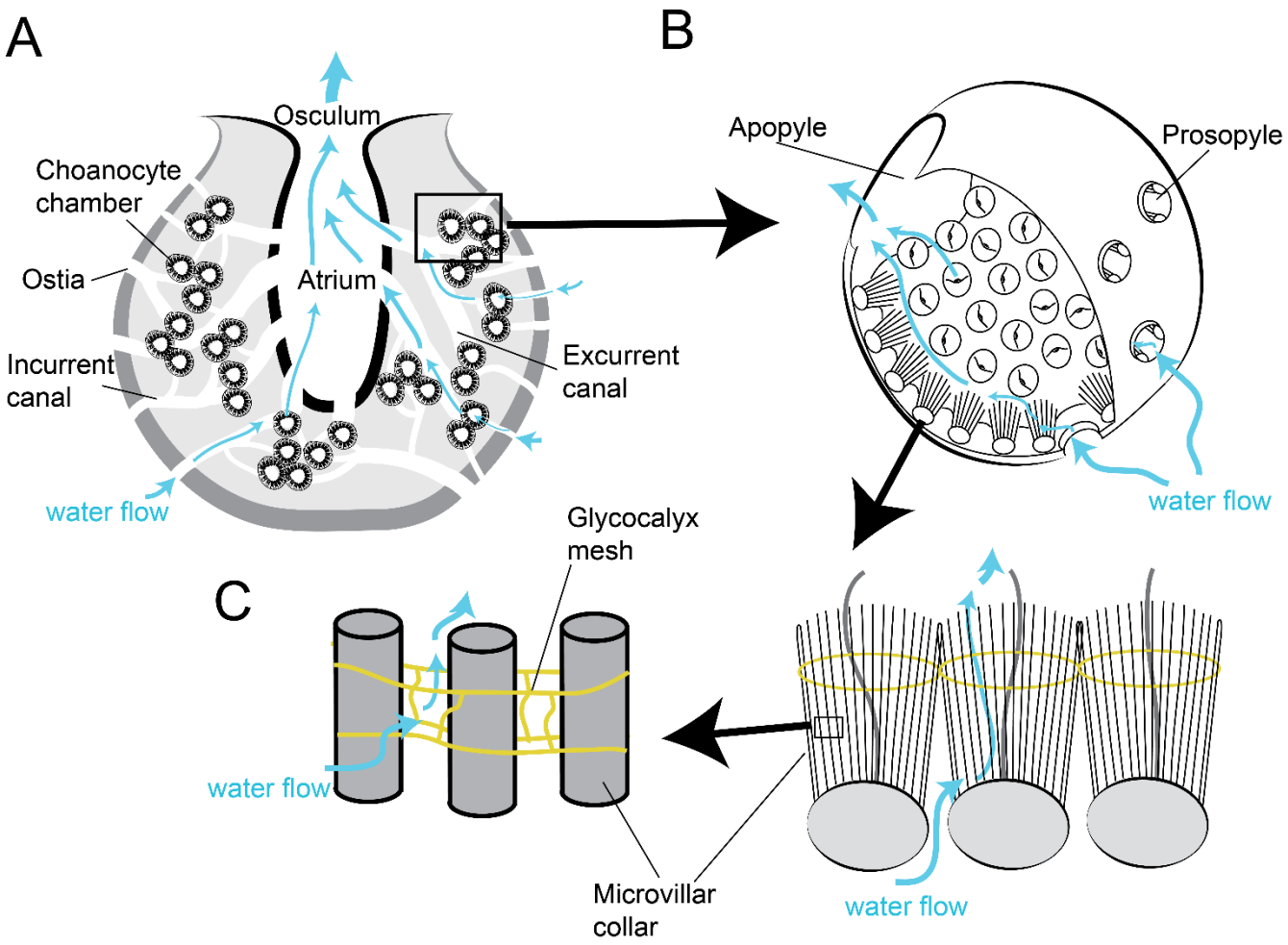

Figure 5| Water flow through the aquiferous canal system of sponges.

Schematic illustrating the path of water through the aquiferous system of sponges. (A) Water enters through pores (ostia) on the sponge surface, into incurrent canals to the choanocyte chambers where the water is filtered, then out through the excurrent canals to the osculum. There is a huge increase in cross-sectional area of the aquiferous system as the water enters the choanocyte chambers, which slows the water for filtration. The cross-sectional area then decreases as the water leaves the choanocyte chambers, jetting the water out through the osculum. (B) Water enters the choanocyte chamber through prosopyles and exits via the apopyle. (C) Glycocalyx (yellow) forms a web that connects all of the collars of choanocyte cells together, such that water passes through the microvilli of the choanocyte chambers. Adjacent microvilli are also connected by a glycocalyx mesh (yellow).

Journal of Experimental Biology • Advance article

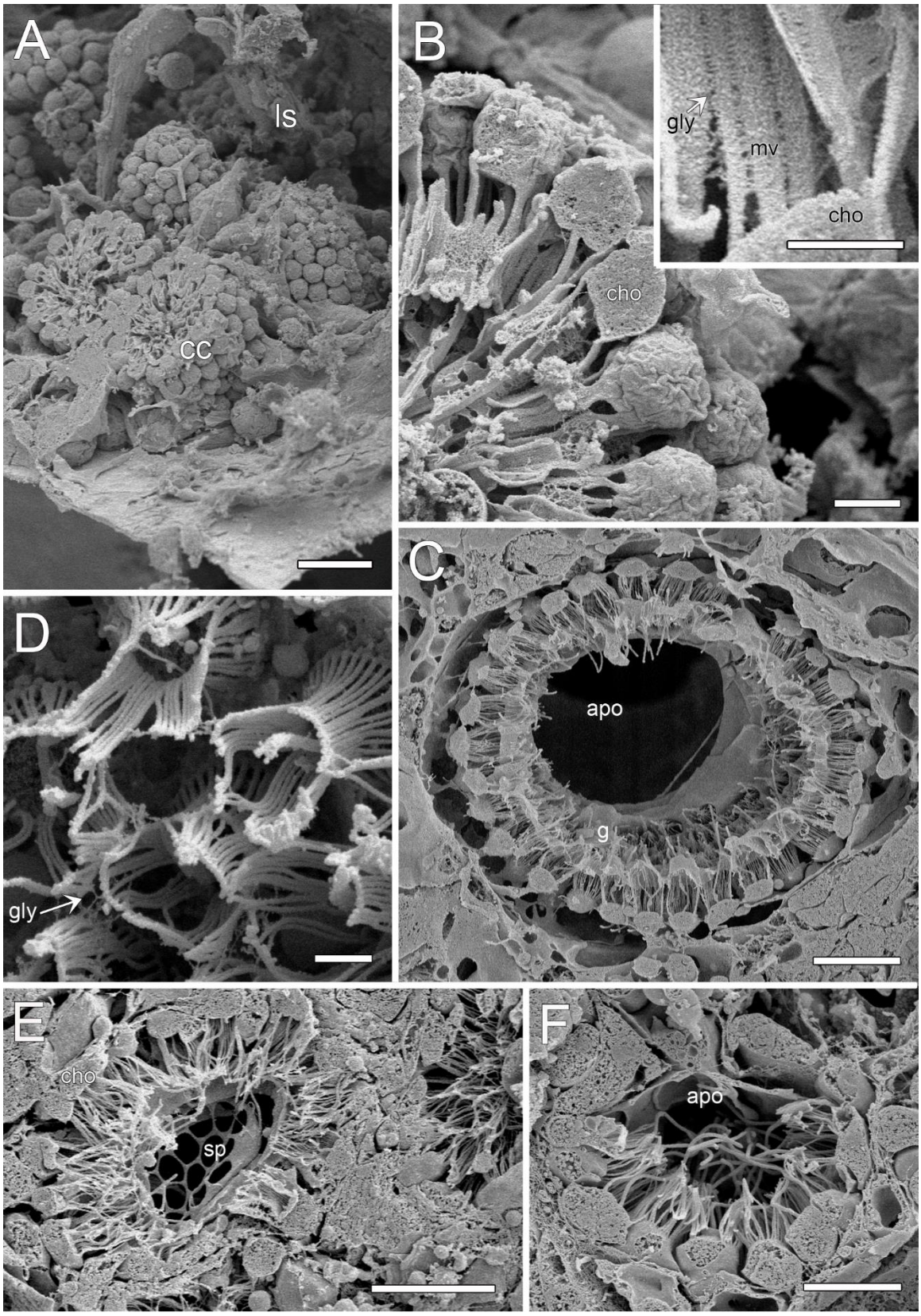

Figure 6| Scanning electron micrographs of choanocyte chambers in five species of demosponges. (A,B) Choanocyte chambers (cc) of *Cliona vaginalis* within the lacunar spaces (ls)**.** Each choanocyte cell (cho) has a collar of microvilli (mv) that are connected by glycocalyx mesh (gly). (C) Large

choanocyte chamber in *Haliclona mollis* showing the cellular gasket (g) that connects each choanocyte cell. Water exits the chamber via the large apopyle (apo). (D) A glycocalyx mesh (gly) connects the collars in *Neopetrosia problematica.* (E) The apopyle in *Tethya californiana* consists of a sieve plate (sp). (F) Smaller choanocyte chamber in *Cliona delitrix* with the flagella protruding from the apopyle. Scale bars A,C,E 10 μm B, 2 μm inset, 1 μm D, 1 μm F, 5 μm

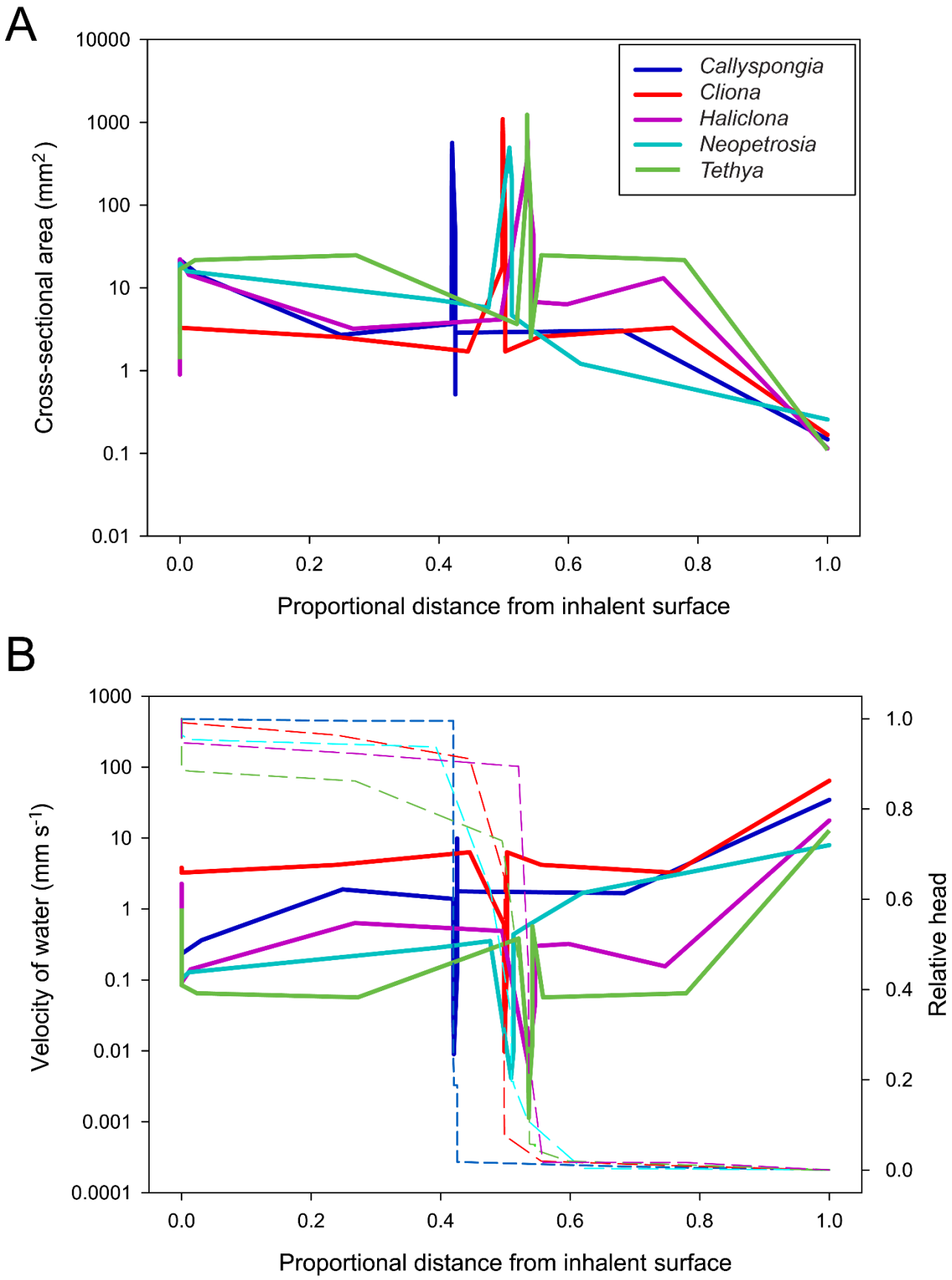

Figure 7| Morphometric model of five species of demosponges. (A) Total cross-sectional area of the aquiferous canal systems (from Table 2) from the inhalant surface to the osculum for five species of demosponges: *Haliclona mollis* (purple), *Neopetrosia problematica* (cyan), *Tethya californiana* (green), *Callyspongia vaginalis* (blue) and *Cliona delitrix* (red**). (B)** Estimated water velocity (solid lines) and relative head loss (dotted lines) through the aquiferous canal system, from Table 3, as water travels from the inhalant surface to the osculum for the same five species of demosponges.

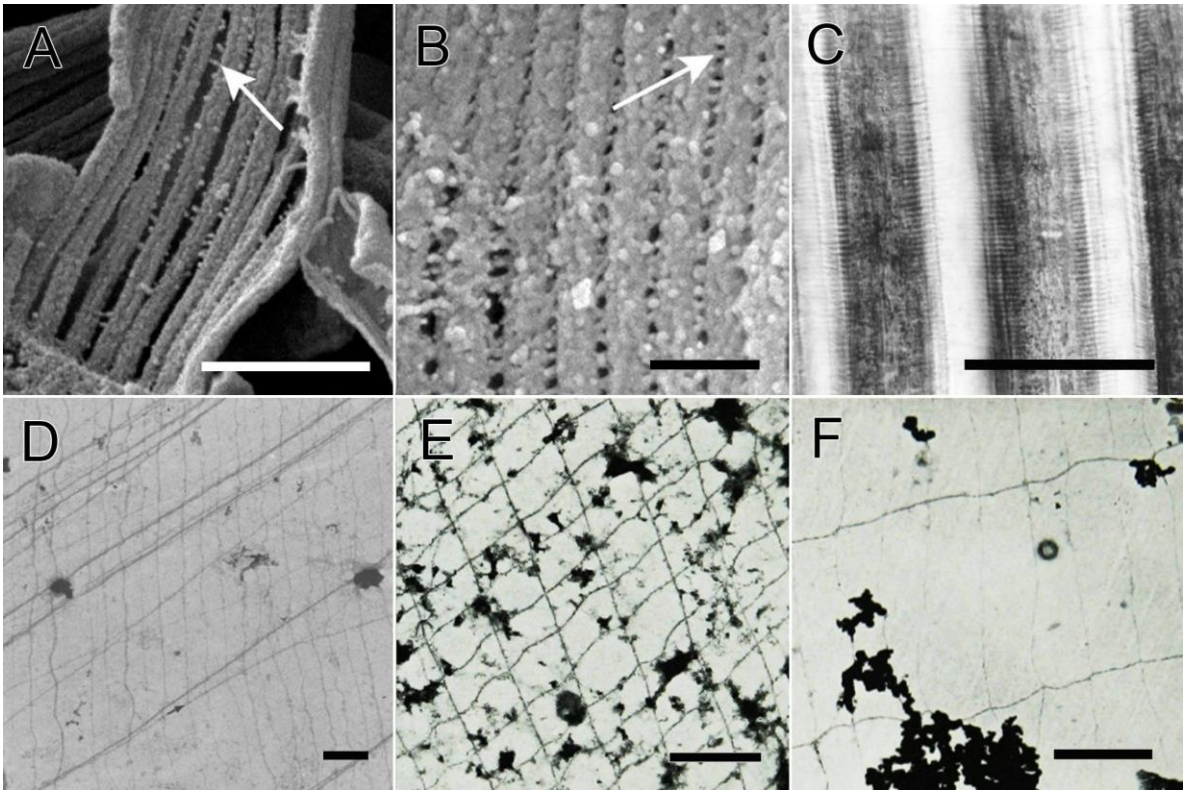

Fig. S1. Feeding filters in four groups of invertebrates used to re-estimate the cost of filtration

(A,B) Scanning electron micrograph (SEM) of the collar of *Spongilla lacustris*, showing the glycocalyx mesh fibrils (arrows) linking adjacent microvilli (Mah et al., 2014) (C) Gill filament of *Mytilus edulis* showing the latero-frontal cirri. (Jones et al., 1992) (D-F) Transmission electron micrographs of the mucus nets in *Chaetopterus variopedatus* (Flood and Fiala-Medioni, 1982) (D), *Ciona intestinales* (Flood and Fiala-Medioni, 1981) (E), and *Styella plicata* (Flood and Fiala-Medioni, 1981) (F) Scale bars (A, D-F) 1 μm (B) 300 nm (C) 100 μm.

Fig. S2. Method of measuring excurrent velocity with the Vectrino Profiler

A) Screen shot (left) of the profiler recording of flow from *Cliona delitrix*. The pink line shows the position of the osculum, just below the osculum lip. The vectors of velocity are: x=yellow, y=red, green and dark blue = two z vectors and pale blue = Vmag (~ scalar). Photo (right) showing the position of the Vectrino Profiler over the osculum of *Cliona delitrix* and the profile. The dashed line shows the position equivalent to the pink line on the figure of the Vectrino record left.

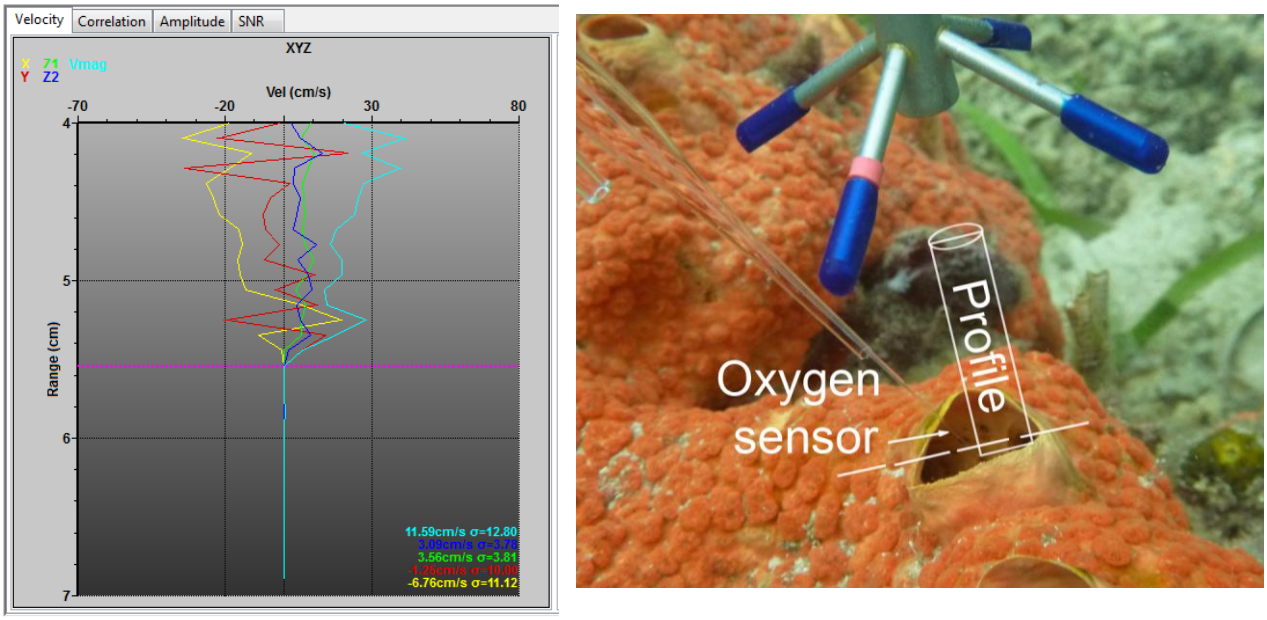

B) Frame grab from a video showing excurrent flow from *Cliona delitrix* (left) and *Callyspongia vaginalis* (right) visualized with fluorescein dye.

Table S1 - Measuring excurrent velocity

- For the cost of pumping we used mean Z (vertical direction only) velocity, measured just at the top of the osculum
- Scalar velocities measured at that same spot varied greatly depending on the ambient flow and the maximum z velocity of each sponge
- For parabolic flow estimate of the 'average' excurrent velocity would use 0.5 x scalar velocity (shown in column D below). To see the effect on cost that number can be inserted in Cell B16 in each of the Species tabs. Using 0.5x scalar velocity reduces the volume pumped for *Cliona* and increases it for *Callyspongia* and *Haliclona*
- We considered that for *Cliona*, for example, the z velocity was the major component of scalar velocity, and therefore it would be a gross underestimate of excurrent velocity to estimate parabolic flow and use 0.5*scalar. In contrast, for *Callyspongia*, the z velocity was lower and the osculum diameter larger, so upon exiting the osculum the ambient flow probably bent the excurrent plume such that scalar velocity grossly overestimated excurrent velocity. (See supplementary videos files of excurrent flow visualized with fluorescein dye.)
- Since we also do not consider the sides of the oscula for all sponges to experience a 'no slip' condition (because water enters the oscula from many canals) there is no other equation to describe the flow across the 'pipe'. Therefore we used the mean Z velocity at Max Z profile to estimate average oscula excurrent velocity

	Effective oscula velocity			Cost of pumping, η (%) Using mean scalar velocity	
	mean Z	mean scalar	0.5 *scalar	Model	
	at max z profile (cm/s)		(cm/s)	Riisgård and Larsen 1993	Leys et al 2011
Cliona delitrix	11	12.7	6.35	8.71	6.81
Callyspongia vaginalis	5.9	18.9	9.45	5.66	8.6
Tethya californiana	2.2	3.5	1.75	0.64	0.6
Haliclona permollis	3	15.3	7.65	4.84	2.59
Neopetrosia problematica	1.3	4	2	5.37	5.78

Table S1 - References

Fiala-Medioni, A. (1978). Filter-feeding ethology of benthic invertebrates (Ascidians). IV. Pumping rate, filtration rate, filtration efficiency. *Marine Biology* **48**, 243-249.

Flood, P. R. and Fiala-Medioni, A. (1981). Ultrastructure and histochemistry of the food trapping mucous film in benthic filter-feeders (Ascidians). *Acta Zoologica* **62**, 53-65.

Flood, P. R. and Fiala-Medioni, A. (1982). Structure of the mucous feeding filter of *Chaetopterus variopedatus*. *Marine Biology* **72**, 27-33.

Grove, M. W., Finelli, C. M., Wethey, D. S. and Woodin, S. A. (2000). The effects of symbiotic crabs on the pumping activity and growth rates of *Chaetopterus variopedatus*. *Journal of Experimental Marine Biology and Ecology* **246**, 31-52.

Jones, H. D., Richards, O. G. and Southern, T. A. (1992). Gill dimensions, water pumping rate and body size in the mussel *Mytilus edulis* L. *Journal of Experimental Marine Biology and Ecology* **155**, 213-237.

Jørgensen, C. B., Famme, O., Kristensen, H. S., Larsen, P. S., Møhlenberg, F. and Riisgård, H. U. (1986). The bivalve pump. *Marine Ecology Progress Series* **34**, 69-77.

Jørgensen, C. B., Larsen, P. S., Møhlenberg, F. and Riisgård, H. U. (1988). The mussel pump: properties and modelling. *Marine Ecology Progress Series* **45**, 205-218.

Mah, J. L., Christensen-Dalsgaard, K. K. and Leys, S. P. (2014). Choanoflagellate and choanocyte collar-flagellar systems and the assumption of homology. *Evolution & Development* **16**, 25-37.

Riisgård, H. U. (1989). Properties and energy cost of the muscular piston pump in the suspension feeding polychate *Chaetopterus variopedatus*. *Marine Ecology Progress Series* **56**, 157-168.

Riisgård, H. U., Thomassen, S., Jakobsen, H., Weeks, J. M. and Larsen, P. S. (1993). Suspension feeding in marine sponges *Halichondria panicea* and *Haliclona urceolus:* effects of temperature on filtration rate and energy cost of pumping. *Marine Ecology Progress Series* **96**, 177-188.

Reiswig, H. M. (1975a). The aquiferous systems of three marine Demospongiae. *Journal of Morphology* **145**, 493-502.

Table S2 - Estimated cost of pumping (%) for four different groups of filter feeders

The cost of pumping (% of metabolism) is based on the morphometric model summarized by Riisgård and Larsen (1995) and outlined in Equations S2-S2 in Box 1, where d = diameter of the cylindrical fiber, b = space between cylinders, h_1 = width of the mesh; h_2 = length of the mesh; and L = length of inter-filament canals. Cost was estimated using new measurements from the literature for filter dimensions and volume flow rates (blue). In the absence of volume flow rates for *Spongilla lacustris*, estimates for *Haliclona permollis* were used instead. Original estimates for the cost of pumping are in black and the new estimates are shown in red.

Species	Filter dimensions (µm)	Filter Dimension Reference	Volume Flow rate (mL min^{-1})	Volume Flow rate Reference	Estimate of the cost of pumping (%)	
Sponges						
Haliclona urceolus	d=0.14, b=0.25	Riisgard et al (1993)	6	Riisgard et al (1993)	**0.850**	
	d=0.14, b=0.25	Riisgard et al (1993)	6	Riisgard et al (1993)	**1.021**	*
Haliclona permollis	d=0.14, b=0.25	Riisgard et al (1993)	18.84	Reiswig (1975)	**3.206**	
Spongilla lacustris	h1=0.048, h2=0.04, d=0.04	Mah et al (2014)	6	Riisgard et al (1993)	**1.594**	
	h1=0.048, h2=0.041, d=0.04	Mah et al (2014)	18.84	Reiswig (1975)	**5.004**	
Bivalves						
Mytilus edulis	L=200, l=40	Jorgensen et al 1986a, 1988	60	Jorgensen et al 1986a, 1988	**1.562**	
	L=200, l=40	Jorgensen et al 1986a, 1988	67.8	Riisgard et al 2011	**1.765**	
	L=200, l=16	Jones et al (1992)	60	Jorgensen et al 1986a, 1988	**4.131**	
	L=200, l=16	Jones et al (1992)	67.8	Riisgard et al 2011	**4.668**	
Polychaetes						
Chaetopterus	h1=2.3, h2=1.4, d=0.02	Riisgard (1989)	18	Riisgard (1989)	**4.032**	
variopedatus	h1=2.3, h2=1.4, d=0.02	Riisgard (1989)	30	Grove et al (2000)	**6.719**	
	h1=0.76 h2=0.46, d=0.02	Flood and Fiala-Medioni (1982)	18	Riisgard (1989)	**10.903**	
	h1=0.76 h2=0.46, d=0.02	Flood and Fiala-Medioni (1982)	30	Grove et al (2000)	**18.172**	
Ascidians						
Styella clava	h1=0.35, h2=1.35, d=0.020	Riisgard and Larsen (1995)	45.6	Riisgard and Larsen (1995)	**0.191**	
	h1=0.35, h2=1.35, d=0.020	Riisgard and Larsen (1995)	45.6	Riisgard and Larsen (1995)	**0.724**	**
Mean of three species	h1=0.35, h2=1.35, d=0.020	Riisgard and Larsen (1995)	57.5	Fiali-Medioni (1978)	**0.913**	
Mean of six species	h1=1.002, h2=0.366, d = 0.025	Flood and Fiala Medioni (1981)	45.6	Riisgard and Larsen (1995)	**0.815**	
Styella plicata	h1=1.959, h2=0.5055, d=0.020	Flood and Fiala Medioni (1981)	83.1	Fiali-Medioni (1978)	**0.885**	
Ciona intestinales	h1=0.640, h2=0.405, d=0.020	Flood and Fiala Medioni (1981)	21.5	Fiali-Medioni (1978)	**0.376**	

* Cost of pumping re-estimated to use consistent temperatures for kinematic viscosity

** Cost of pumping re-estimated using corrected head loss at the filter

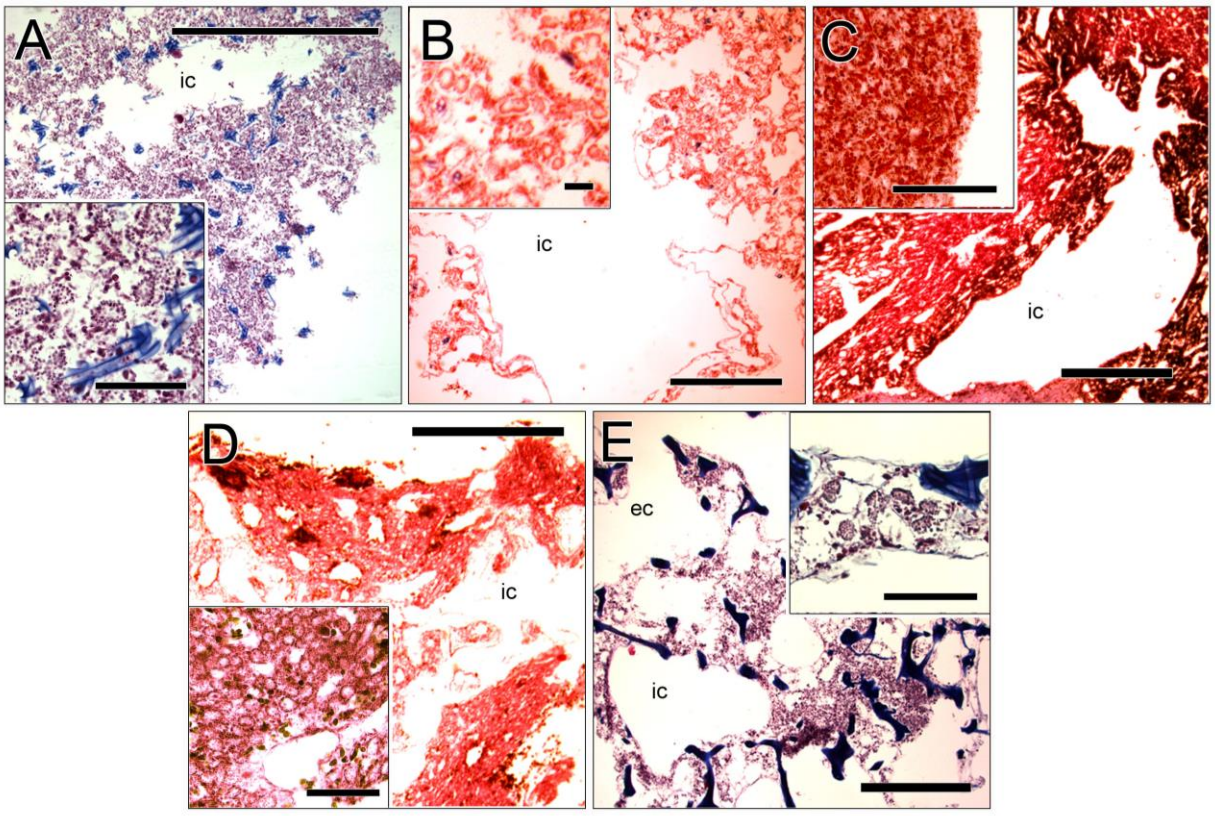

Fig. S3. Histological sections in five species of demosponges| Histological sections in five species of demosponges. Incurrent (ic) and excurrent (ec) canals in (A) *Neopetrosia problematica* (B) *Haliclona mollis* (C) *Tethya californiana* (D) *Cliona delitrix* (E) and *Callyspongia vaginalis.* Insets show choanocyte chambers. Scale bars: 1 mm; insets: 100 μm